Stiffness of Central Current and Temperature Profiles in JT-60U Current Hole Plasmas

T. Fujita, T. Suzuki, T. Oikawa, S. Ide, Y. Sakamoto, H. Takenaga, A. Isayama, T. Hatae, O. Naito, N. Hayashi, K. Hamamatsu, T. Takizuka, Y. Miura and the JT-60Team

Japan Atomic Energy Research Institute, Naka Fusion Research Establishment
Naka-machi, Naka-gun, Ibaraki-ken, Japan.

e-mail contact of main author: fujitat@fusion.naka.jaeri.go.jp

Abstract. In JT-60U, the response of current density and electron temperature profiles in the central region to current drive and local heating was investigated in plasmas with and without a current hole. We found that no toroidal current was driven, by inductive electric field, electron cyclotron wave current drive and neutral beam current drive, in the current hole region in spite of high electric conductivity. The electron temperature profile remained nearly flat even with intense localized heating in plasmas with strong ITBs, both with and without a current hole. These results, namely stiff current and temperature profiles, suggest that there is a mechanism to clamp the current density and the temperature gradient nearly zero in the current hole and/or inside the ITB layer.

1. Introduction

In an extreme situation of the hollow current profile, it was found that there is no plasma current in the central region (called "current hole") in JT-60U and JET [1,2]. In JT-60U, the current hole exists stably for several seconds [3]. Though temperature and density profiles were nearly flat in the current hole, internal transport barriers (ITBs) were formed outside the current hole, and high temperature plasmas were confined in the current hole. Our concern is whether these profiles, small current density and temperature gradients, are the results of small driving force (current drive and heating) or are maintained by some damping mechanism against the driving force. To address this issue, we applied current drive and/or local heating into the current hole to enhance the driving force and investigated responses of current density and electron temperature.

2. Current Clamp in the Current Hole

The cause of current hole formation is considered to be off-axis non-inductive current, for instance, the bootstrap current in the ITB layer in JT-60U [3] and the current driven by a lower hybrid wave in JET [2]. The toroidal electric field $E_\phi(0)$ and hence $j(0)$ are decreased by the increase of the off-axis non-inductive current through the Faraday's law, and the current hole is finally formed. This process can lead to a negative $j(0)$ in principle, but no significant negative $j(0)$ has been observed so far. This fact suggests that the decrease in $j(0)$ stops when it becomes zero. A resistive kink instability was proposed to explain the absence of negative $j(0)$ [4, 5]. In this model, $j(0)$ does not become negative but is clamped at zero (current hole is maintained) so long as $E_\phi(0)$ is negative, and $j(0)$ becomes positive (current hole disappears) when $E_\phi(0)$ becomes positive. However, the measurement of $E_\phi(\rho)$ (ρ is the normalized minor radius) in the current hole was not done in experiments so far. In this section, we present $E_\phi(0)$ measurements and existence of current clamp in the current hole both for the positive direction as well as for the negative direction.

Three kinds of experiments were performed to investigate response of the current hole to inductive toroidal electric field and that to non-inductive current drive separately.

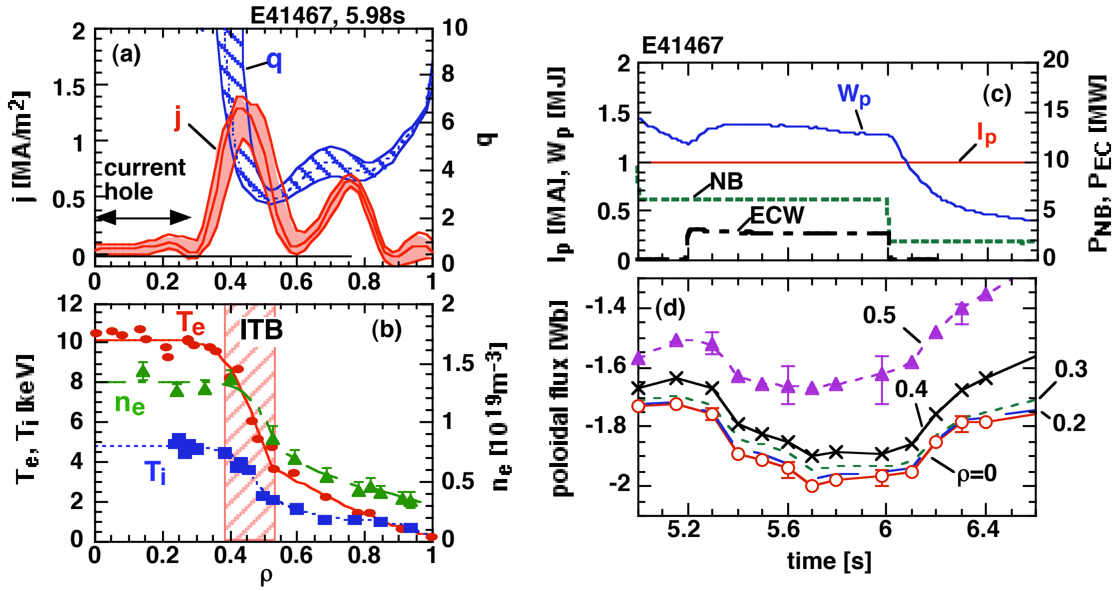

FIG. 1. Response to change of inductive electric field of a current hole plasma (E41467). (a) Radial profiles of current density (j) and safety factor (q). (b) Radial profiles of electron temperature (T_e), ion temperature (T_i) and electron density (n_e). (c) Waveforms of plasma current (I_p), plasma stored energy (W_p), injected NB power (P_{NB}), and injected EC power (P_{EC}). (d) Time evolution of poloidal flux at ρ = 0, 0.2, 0.3, 0.4 and 0.5.

In the first experiment (shot E41467), shown in Fig. 1, the inductive toroidal electric field was changed transiently keeping the non-inductive current inside the current hole as small as possible. The neutral beam (NB) units were selected to minimize the beam-driven current in the current hole; 1 MW for co- and counter- tangential units and 4 MW for nearly perpendicular units for t = 5-6 s. A current hole plasma with ITBs was established by NB heating during the current ramp. The plasma major radius (R_p) was 3.35 m, the plasma minor radius was 0.7 m, the plasma current (I_p) was 1 MA, the toroidal field at R_p (B_t) was 3.6 T, and the safety factor at 95% of poloidal flux (q_{95}) was ~6. At t = 5.2 s, an electron cyclotron wave (ECW) of 2.6 MW, 110 GHz was injected so as to be absorbed outside the current hole to increase the non-inductive current, EC-driven current and bootstrap current, in the same direction to the plasma current. At t = 6.0 s, ECW power and almost all NB power were stopped, except NBs for the MSE (Motional Stark Effect) measurements, to decrease the non-inductive current rapidly. We can obtain the radial profile of toroidal loop voltage $V_{loop}(\rho)$ from the time-derivative of poloidal flux $\Psi(\rho)$ [6]; $V_{loop}(\rho) = d\Psi(\rho)/dt$ and $E_\phi(\rho)$ is given by $E_\phi(\rho) = V_{loop}(\rho)/(2\pi R_p)$. Here $\Psi(\rho)$ is obtained from the equilibrium reconstruction.

Here, an equilibrium with a single axis and with a sufficiently high q(0) (small j(0)) is reconstructed to model the current hole plasma. Though some models predict existence of magnetic islands with toroidal symmetry [7, 8], the poloidal field in such structures, if any, is too small to be measured in the present MSE diagnostic. $\Psi(\rho)$ and $E_t(\rho)$ hardly depend on models of the structure of the current hole because of sufficiently small B_p in the current hole. The uncertainties in j and q originate from the systematic calibration errors and statistical errors in polarization angle measurements and uncertainties in the pressure profile that changes the location (Shafranov shift) and shape of flux surfaces.

The time evolution of poloidal magnetic flux at several locations is shown in Fig. 1 (d). The poloidal magnetic flux near the axis decreased during ECW injection and increased after decrease of NB and ECW powers, as intended. The current hole was maintained during the

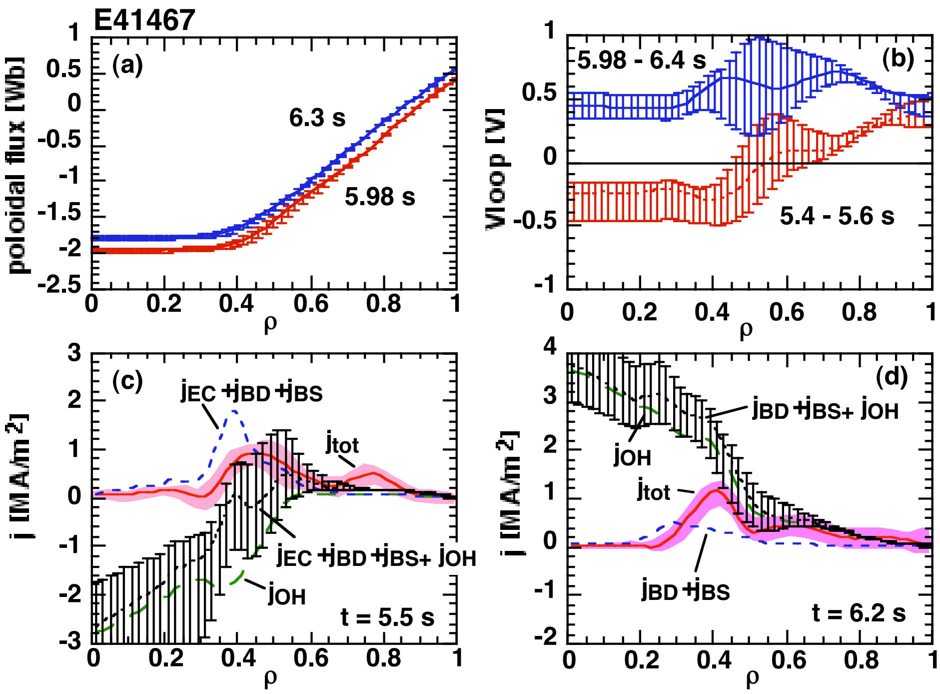

FIG. 2. Radial profiles in E41467. (a) Radial profiles of poloidal flux at t = 5.98 s and 6.3 s. (b) Radial profiles of loop voltage (V_{loop}) during t = 5.4-5.6 s and t = 5.98-6.4 s. (c),(d) Radial profiles of current density at (c) t = 5.5s and (d) t = 6.2 s. In (c) and (d), j_{tot} (solid line with a shaded belt) denotes measure current density, j_{OH} is calculated inductive current density, j_{EC} is calculated ECW-driven current density, j_{BD} is calculated beam-driven current density and j_{BS} is calculated bootstrap current density. The sum of $j_{OH} + j_{BD} + j_{BS} + j_{EC}$ is shown by a dotted line with error bars.

period shown in the figure, as indicated by nearly the same trajectories of Ψ(0) and Ψ(0.2) that mean negligible poloidal field inside ρ = 0.2.

In Fig. 2 (a) and (b), radial profiles of Ψ(ρ) and V_{loop}(ρ) are shown. The profile of Ψ(ρ) is nearly flat in the current hole due to a small poloidal field there and starts to increase outside the current hole. Larger uncertainties in V_{loop}(ρ) are found around ρ ~ 0.5 but uncertainties are relatively small near the center. This is because the poloidal field measurements are done at fixed position in space not in ρ, so that the uncertainties in the pressure profile or in the Shafranov shift causes errors in Ψ(ρ) where it has a large gradient. The V_{loop}(0) was negative (~ -0.3 V) during t = 5.4-5.6 s while it was positive (~ +0.4 V) during t = 5.98-6.4 V. The ohmic current density j_{OH} at the center expected from these values of V_{loop}(0) was - 2.6 MA/m^2 and + 3.6 MA/m^2, respectively. The beam-driven current is estimated by orbit following Monte Carlo code (OFMC) [9] and is found less than 0.2 MA/m^2 and negligible in the current hole. The ECW-driven current j_{EC} is evaluated by a linearized Fokker-Planck code with ray-tracing [10] and is found located outside the current hole as intended. The bootstrap current j_{BS} is calculated from the pressure and q profiles, where the pressure is given by the sum of thermal component and beam component, the latter of which is estimated by the OFMC code. Since the bootstrap current is proportional to the pressure gradient divided by B_p, its evaluation accompanies large errors near and in the current hole where B_p is very small. The bootstrap current is expected to be small in the current hole from the observation that temperature and density profiles are nearly flat in the current hole as shown in Fig. 1 (b), but it depends on how fast pressure gradient approaches zero as B_p approaches zero. Here, j_{BS} is assumed zero in the region inside ρ = 0.2 in current hole plasmas. In Fig. 2 (c) and (d), the sum of calculated j_{OH}, j_{EC}, j_{BD} and j_{BS} is shown in dotted lines with error bars while measured j_{tot} is shown by solid lines with a shaded belt. In both cases, the calculated current density is dominated by inductive current and is largely negative at t = 5.5 s and is largely positive at t = 6.2 s. The measured current density, however, remained nearly zero. This indicates that the current density in the current hole is kept nearly zero against large driving force both in positive and negative directions.

In the second experiment, ECW current drive (ECCD) inside the current hole was attempted in the positive (co) and negative (counter) directions during the quasi-stationary period in two discharges (E41735 and E41777). The waveforms for co-ECCD case (E41735) are shown in Fig. 3 (a)-(c). The configuration and plasma current were similar to E41467, but the toroidal field was slightly higher (3.7 T). The ECW of 2.6 MW, 110 GHz was injected during t = 5.2-6.0 s. In Fig. 3 (b), measured current density in the central region (averaged inside ρ = 0.2) and calculated current density driven by ECW are shown. The measured current density remained nearly zero (~0.05 MA/m^2) though a large current density (>~ 1 MA/m^2) is expected by ECCD. The time evolution of Ψ(ρ) is shown in Fig. 3 (c). Though Ψ(0) decreased and the negative $V_{loop}(0)$ was generated for the first 0.5 s of ECW injection, Ψ(0) stayed nearly constant for t = 5.7-6.0 s. The current hole was maintained after turn-off of ECW though its radius became smaller than 0.2 at t = 6.8 s as shown in Fig. 3 (b) and finally disappeared at t ~ 7.2 s. It is noted that positive $E_\phi(0)$ is also generated in this discharge after the turn-off of ECW, during t = 6-6.3 s, as indicated by increase in Ψ(0), and the current hole was maintained against the positive $E_\phi(0)$. Radial profiles of measured and calculated current density are shown in Fig. 3 (d) and (e) for co and counter cases, respectively. In both cases, the inductive electric field was sufficiently small and the beam-driven current is also small in the current hole. Hence the ECW-driven current should emerge in its original shape if the bootstrap current is sufficiently small as assumed. It is noted that in the code for ECCD evaluation [10], the displacement (drift) of electron orbit from the magnetic surface is neglected. Though the displacement of electron orbit from the magnetic surface is sufficiently small (a few cm) even in the equilibrium with very high q(0) (~100),

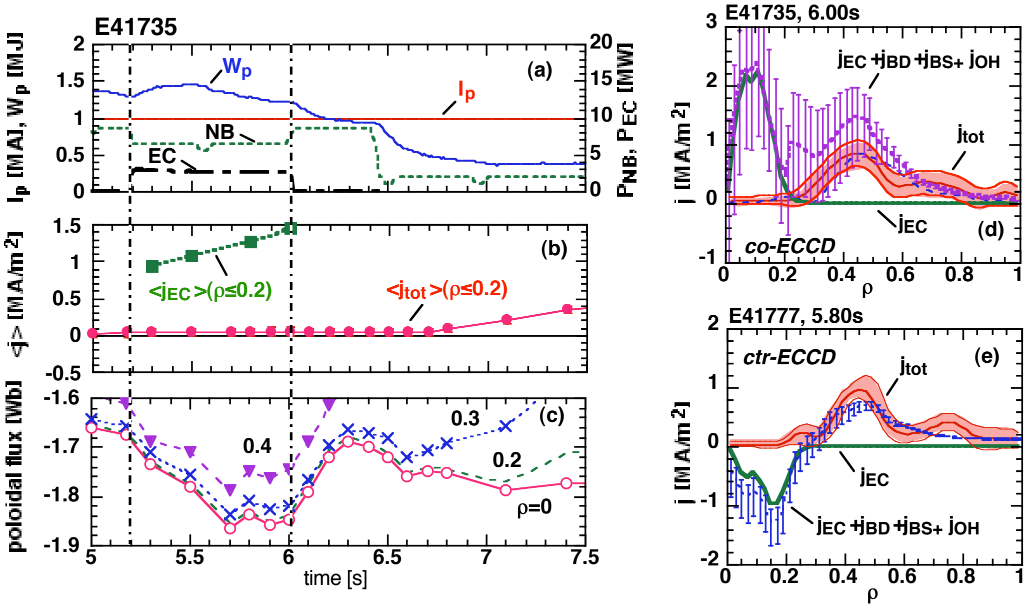

FIG. 3. Response to ECW-driven current of current hole plasmas. (a)-(c) Waveforms for the co-ECCD case; (a) plasma current (I_p), plasma stored energy (W_p), injected NB power (P_{NB}), and injected EC power (P_{EC}), (b) current density in the central region (ρ≤0.2) for ECW-driven current and measured total current, and (c) poloidal flux. (d)-(e) Profiles of current density for (d) the co-ECCD case and for (e) the counter-ECCD case.

the orbit can expand the whole current hole region if q(0) is much higher or is infinite. In such a circumstance, the EC-driven current is supposed to fill the current hole uniformly and its shape may be different from that shown in Fig. 3 but it should still appear. On the other hand, measured current density was nearly zero in both cases. This indicates that the EC current drive did not change the current inside the current hole and the current hole was maintained.

In the third experiment, response to NBCD was investigated. Negative ion based NB (NNB) with 370 keV, 3.1 MW was injected into a central region of a current hole plasma with I_p = 0.8 MA, B_t = 2.9 T, q_{95} ~ 7. Neon gas was injected 0.3 s after the start of NNB injection (t = 5.3 s) to raise Z_{eff}. Higher Z_{eff} enhances the beam driven current, if T_e and n_e are unchanged, and reduces the errors of estimation of inductive current by reducing the conductivity. The current hole was maintained until t = 8.8 s or 2.5 s after the NNB injection. The loop voltage in the central region stayed nearly constant for t = 6-7.2 s. The profiles of measured and calculated current density at t = 6.4 s are shown in Fig. 4. The beam-driven current was estimated by using the OFMC code [9], which treats the fast ion orbit correctly in a weak poloidal field region in the current hole plasma. The current driven by NNB is 0.27 MA and that by conventional positive ion based NB (PNB) was 0.11 MA. The current density for the total beam driven current was 0.33 MA/m^2 and the inductive current density was ~0.05 MA/m^2 in the central region as shown in Fig. 4. The measured current density, j_{tot}, however, is very low (~0.05 MA/m^2). This indicates that the NBCD is ineffective in the current hole.

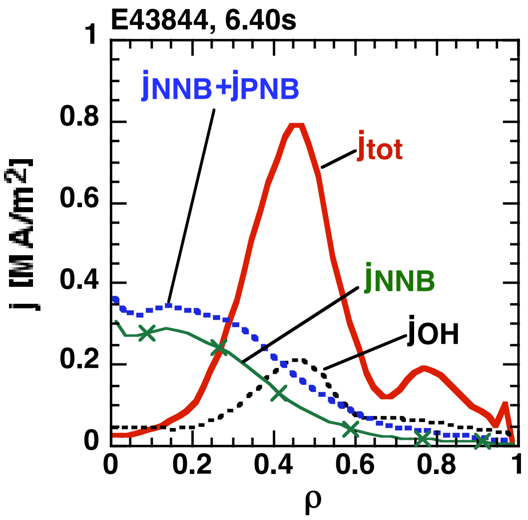

FIG. 4. Current profile for an NBCD case.

From these results, it has been shown experimentally for the first time that the current hole is not maintained by the fact that the current drive source remains zero in the current hole but by some mechanism to clamp the current density at zero level once when the current density becomes at zero level in the central region. Some simulation results show that resistive MHD instabilities take place in the current hole and they work for the current clamp [4, 5]. In our experiments, however, no MHD instabilities were observed inside and just outside the current hole. This indicates that the current hole is not maintained by repeated instabilities but some stationary state with the current hole was realized. Another very important difference is that current clamp was observed only for the counter direction in the simulation but in both co and counter directions in the experiment. In other words, the current hole behaves like a diode in the simulation, but like an insulator inside the highly-conductible plasma in the experiment. We have two possible candidates, which cause differences in the calculated and measured current densities in the current hole. The first one is the bootstrap current, which has been assumed zero in the current hole. Since the poloidal field is small in the current hole, a small pressure gradient below the measurement limit can generate a large bootstrap current. The second one is the electric field induced by radial flow across remaining small poloidal field (v x B field). This is important in the magnetic reconnection region near the field null point (X point), where plasma flow across the field line can be generated, and a similar situation may exist in the current hole region with a small poloidal field. In both cases, the important point is that these seem to work so as to keep the current density nearly zero automatically. Namely, the current hole is one of self-organized structures in a torus plasma. The mechanism to realize this state is not yet known.

3. Temperature Profile

In reversed shear plasmas with strong ITBs, a box-type shape of density and temperature profiles is often observed, where a flat portion exists around the axis or inside the ITB layer (steep gradient region) [11]. The point connecting the flat portion and the steep gradient region is called an ITB 'shoulder.' One may suppose that the appearance of the flat portion, which implies very poor confinement there, is related to the existence of current hole. Flat regions in these profiles, however, are observed even before the current hole formation, which indicates that the flat profiles are not directly related to the current hole. The flat T_e profile with a peaked T_i profile was observed in DIII-D negative central shear discharges without a current hole, and the cause of enhanced electron transport was not identified [12]. Local heating in the flat T_e region was performed using an EC wave to see if these flat profiles are stiff or not.

Figure 5 shows response of electron temperature profile $T_e(\rho)$ to EC heating localized near the axis. Three discharges are compared: (a) a current hole plasma with box-type ITBs, (b) a plasma with box-type ITBs but without a current hole, and (c) a plasma without strong ITBs and without a current hole. Flat $T_e(\rho)$ is observed for all three discharges before EC heating as shown by dotted line with crosses. In the current hole plasma, the flat $T_e(\rho)$ was maintained during EC heating as shown in Fig. 5 (a). In a plasma without strong ITBs and without a current hole, $T_e(\rho)$ became peaked during EC heating as shown in Fig. 5 (c). In a plasma with strong ITBs but without a current hole, the flat T_e profile was maintained as shown in Fig. 5 (b). In (a) and (b), the electron heating power inside $\rho = 0.3$ was increased fivefold with EC heating, but the T_e profile remained nearly flat, which means strong profile

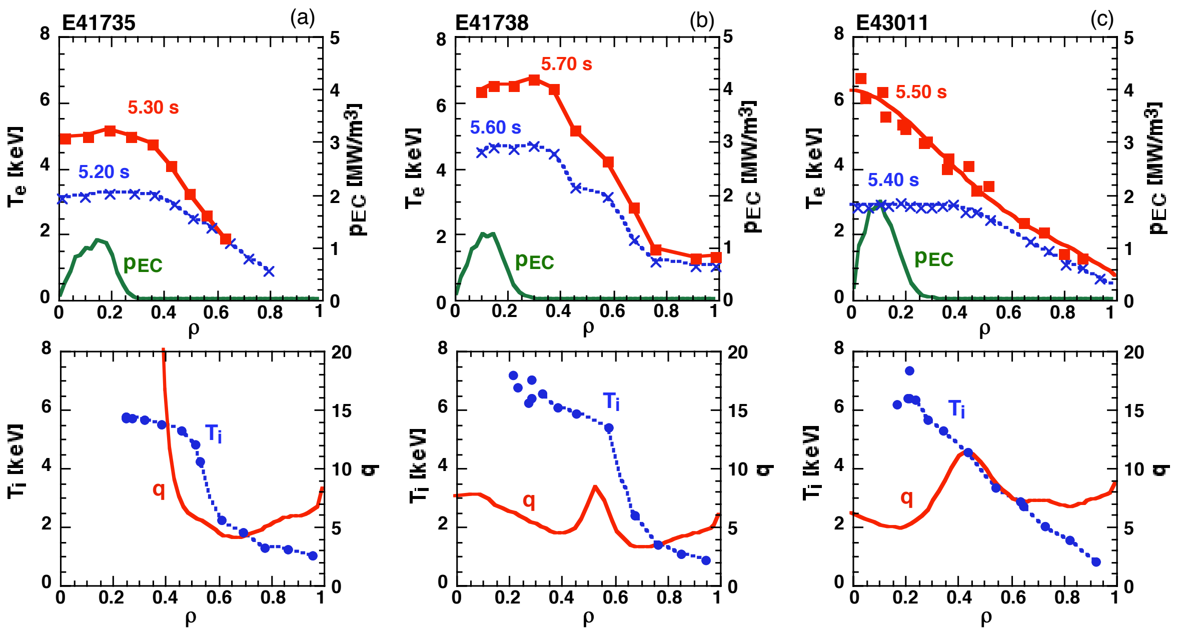

FIG. 5. Response to EC heating localized near the axis. Top: T_e profiles just before and 60-100 ms after the start of EC heating and EC heating profile. Bottom: T_i and q profiles. (a) A current hole plasma with box-type ITBs (I_p = 1MA, Bt =3.7 T, P_{EC} = 2.6 MW). (b) A plasma with box-type ITBs and without a current hole (I_p = 1.3 MA, Bt =3.7 T, P_{EC} = 2.6 MW). (c) A plasma without a strong ITB and without a current hole (I_p = 0.9 MA, Bt =3.7 T, P_{EC} = 2.2 MW).

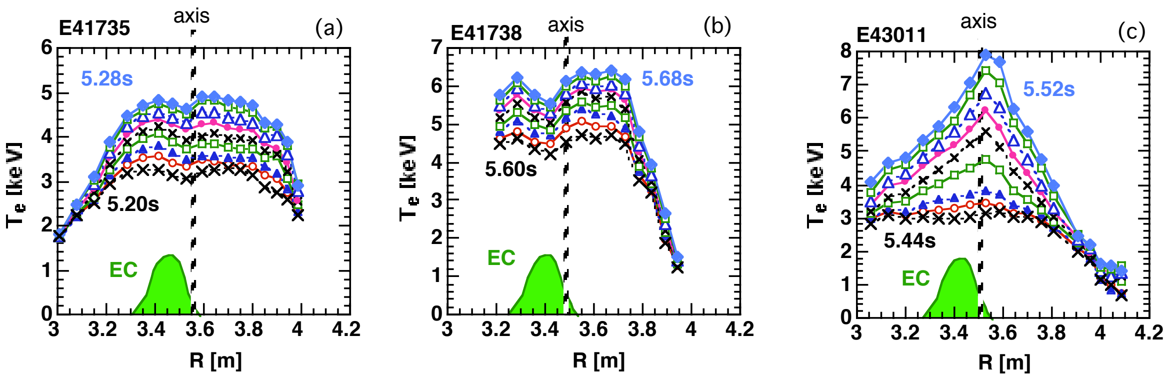

FIG. 6. Time evolution of electron temprature profile along the major radius for the same discharges in Fig. 5.

stiffness. The evolution of T_e profile is shown in Fig. 6 for the same discharges. In (c), peaking of $T_e(\rho)$ starts within 30 ms after the start of EC heating, while in (a) and (b), T_e in the flat region starts to rise almost simultaneously, which indicates very fast heat transport in this region.

From these results, it has been shown that the flat and stiff T_e profile is formed in the central region inside the layer of strong ITBs regardless of existence of current hole.

4. Summary and Discussion

The response of current density and electron temperature profiles in the central region to current drive and local heating was investigated in plasmas with and without a current hole. In the current hole region, no toroidal current was generated by inductive electric field, electron cyclotron wave current drive and neutral beam current drive, and some mechanism exists to clamp the current at zero level. The electron temperature profile remained nearly flat even with intense local heating in the central region of strong ITB plasmas with and without a current hole. The stiffness of temperature profile in a plasma without a current hole suggests that the flat temperature profile is not due to a low poloidal field but due to anomalous transport that arises with a very small temperature gradient.

Acknowledgements

The authors wish to express their thanks for the continuous efforts of the engineering and technical staff at JAERI contributing to the JT-60U project. They also thank Prof. K. Toi in NIFS for valuable suggestions for the experiment. This work was partly supported by Grant-in-Aid for Scientific Research from the Japan Society for the Promotion of Science.

References

[1] IDE, S. and JT-60 TEAM, J. Plasma and Fusion Research SERIES **4** (2001) 99.
[2] HAWKES, N. C., et al., Phys. Rev. Lett. **87** (2001) 115001.
[3] FUJITA, T. et al., Phys. Rev. Lett. **87** (2001) 245001.
[4] HUYSMANS, G. T. A., et al., Phys. Rev. Lett. **87** (2001) 245002.
[5] BRESLAU, J. A., et al., Phys. Plasmas **10** (2003) 1665.
[6] FOREST, C. B., et al., Phys. Rev. Lett. **73** (1994) 2444.
[7] TAKIZUKA, T., J. Plasma Fusion Res. **78** (2002) 1282.
[8] MARTYNOV, A. A., and MEDVEDEV, S. Yu., Phys. Rev. Lett. **91** (2003) 085004.
[9] TANI, K., et al., J. Phys. Soc. Jpn. **50** (1981) 1726.

[10] HAMAMATSU, K., et al., Fusion. Eng. Des. **53** (2000) 53.
[11] SHIRAI, H., et al., Nucl. Fusion **39** (1999) 1713.
[12] STALLARD, B. W., et al., Phys. Plasmas **6** (1999) 1819.